ISSN 2075-1133, Inorganic Materials: Applied Research, 2019, Vol. 10, No. 4, pp. 999–1002. © Pleiades Publishing, Ltd., 2019.
Russian Text © The Author(s), 2019, published in Materialovedenie, 2019, No. 2, pp. 34–37.

The Influence of CuO Dopant Nanoparticles, Prepared via the Arc Plasma Synthesis Method, on the Critical Current of $YBa_2Cu_3O_{7-\delta}$ Composites

A. V. Ushakov[a, b, *], I. V. Karpov[a, b], A. A. Lepeshev[a, b], M. I. Petrov[c], L. Yu. Fedorov[b], D. M. Gokhfel'd[c], S. M. Zharkov[b, c], G. M. Zeer[b], V. G. Demin[b], and A. K. Abkaryan[b]

[a] *Federal Research Center Krasnoyarsk Scientific Center, Siberian Branch, Russian Academy of Sciences, Krasnoyarsk, 660036 Russia*

[b] *Siberian Federal University, Krasnoyarsk, 660041 Russia*

[c] *Kirensky Institute of Physics, Siberian Branch, Russian Academy of Sciences, Krasnoyarsk, 660036 Russia*

**e-mail: sfu-unesco@mail.ru*

Received January 11, 2018; revised April 17, 2018; accepted July 31, 2018

Abstract—$YBa_2Cu_3O_{7-\delta}$–CuO composites with CuO particle contents of 0.5, 1.0, 2.0, 5.0, 10, 15, 20, and 24% were produced via arc plasma synthesis. Their magnetic properties were analyzed in the context of the expanded critical state model. In comparison with a reference sample, the critical current intragranular density increased in composites with CuO concentrations of 0.5, 1, 20, and 24%. The mechanisms of the influence of nanodopants on the change in the critical current density at various volume contents of nano-CuO were proposed as well.

Keywords: nanodispersed powder, high-temperature superconductor, copper oxide, vacuum arc

DOI: 10.1134/S2075113319040439

INTRODUCTION

The critical current density J_c is an important characteristic of a superconducting material in practical applications. This quantity describes the maximum electric current passing through a superconductor with no energy dissipation at the given temperature and magnetic field. In type-II superconductors (all high-temperature superconductors (HTSC)), the energy dissipation occurs owing to the Abrikosov vortices on account of their interaction with a transport current or the screening currents in a superconductor. The movement of vortices may be substantially reduced via the creation of Abrikosov vortex pinning centers. Since the Abrikosov vortex diameter is comparable with the double coherence length, the preferable pinning center size for HTSCs is several tens of nanometers. The problem of the creation of pinning centers in HTSCs, as well as their thermal and chemical stability, is thoroughly described in the literature [1–5].

The study of transport properties of HTSC + CuO composites simulating the network of weak S–I–S bonds revealed that the chemical interaction of $YBa_2Cu_3O_7$ with CuO is negligibly weak [6]. The development of the arc plasma method for the synthesis of CuO nanoscales aroused interest in the investigation of the effect of CuO nanoinclusions on the transport properties of superconducting $YBa_2Cu_3O_7$ polycrystals.

EXPERIMENTAL

Artificial pinning centers were created by using CuO nanodispersed powders with a characteristic granule size below 10 nm. The CuO nanopowder was synthesized in a plasma chemical reactor in accordance with a technique described in [7, 8]. The arc evaporator used in the synthesis exhibited the following characteristics: the pulse arc discharge current was 2.3 kA and the strength of the longitudinal magnetic field on the cathode surface, generated by the coil, was 80 mT. The sputtering cathode was technically pure copper. In order to activate the plasma chemical reactions, the chamber was purged with a 10% O_2 + 90% Ar gas mixture after the pre-evacuation to a pressure of 1 mPa. The synthesis was conducted at a pressure of 10 Pa. Before the evaporation, the cathode was heated to 700 K. The copper oxide nanopowder had a black color. The weight concentrations of dopants were 0–24 wt %.

$YBa_2Cu_3O_{7-\delta}$ specimens with various CuO nanoparticle contents were produced in accordance with a conventional ceramic technology. A mixture of $YBa_2Cu_3O_{7-x}$ powders and CuO nanoparticles was

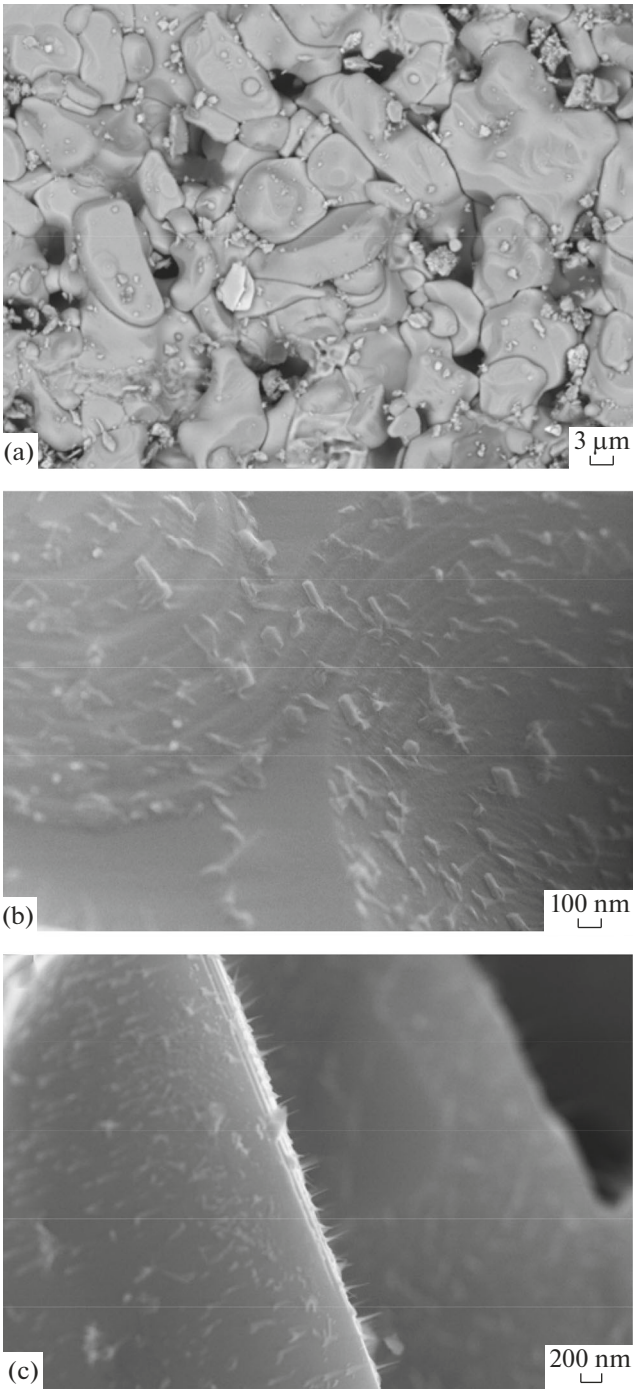

Fig. 1. Microstructure of CuO–$YBa_2Cu_3O_{7-x}$ at various CuO contents: (a) 10; (b) 15; (c) 20 wt %.

stirred in a rotating container for 30 h with a successive cold pressing into cylindrical tablet samples with a diameter of 1 mm and length of 7 mm. The pressing pressure for all samples was equal, being 10 MPa. The subsequent high-temperature sintering of various tablets, including the dopant-free sample, was conducted concurrently at a temperature of 840°C for 10 h.

The structural studies of samples were conducted via scanning electron microscopy on a JEOL JSM-7001F electron microscope at the Center for Shared Use (Siberian Federal University).

The comprehensive analysis of the field magnetization dependence of $YBa_2Cu_3O_{7-\delta}$ compounds with different CuO contents was conducted on a MPMSXL Quantum Design (USA) SQUID magnetometer in a magnetic field up to 9000 Oe at nitrogen temperature. The critical current density of samples was evaluated by using the expanded critical state model [9] from the magnetization loops.

RESULTS AND DISCUSSION

The magnetization loop of a polycrystalline superconductor is determined by the currents circulating across the specimen and granules. The intergranular current, whose density is equal to the transport critical current density, makes a contribution to the magnetization only in magnetic fields below 100 Oe [10]. In severe fields, the superconductivity of intergranular boundaries is completely suppressed by the magnetic field, and the magnetic properties of a polycrystalline specimen are determined by the magnetization of granules. Hence, the average intragranular critical current density can be found from the magnetization loops, measured in high enough fields. The relationship between the critical current density J_c and the nonequilibrium magnetization of the sample ΔM is defined by the Bine formula

$$J_c = 3\Delta M/2R,$$

where R is the current circulation radius (in this case, the average granule radius).

It has to be mentioned that structural parameters of samples, such as density, porosity, and granule size, may exert influence on the J_c values of samples and must therefore be taken into consideration.

For all specimens, the linear segment of the initial magnetization from $H = 0$ to $H = H_{c1}$ has the same slope (in the case of the volume magnetization of the superconductor granules), which testifies to the equal density of granules. The average granule radius was found from the optical micrographs of samples (Fig. 1a) to be $R = 1.9$ μm by means of the random secant method. Meanwhile, because of the large size distribution, the average granule size may slightly vary from this value for various samples. The more accurate evaluation of R can be obtained from the asymmetry of the magnetization loop relative to the H axis. The measured magnetization loops exhibit different asymmetry, and the degree of asymmetry of the magnetization curve is determined by the surface area depth with equilibrium magnetization to the granule radius. The depth of the surface area l is equal to the penetration depth of the magnetic field λ. We estimate the l/R ratio from the degree of asymmetry of the loop. For this, we

use the value $\lambda = 200$ nm for YBCO. As follows from the expanded critical state model, $J_c = j_c(1 - 1/R)^3$, where j_c is the critical current density of a sample with $R \gg \lambda$. For a sample with $R \gg \lambda$, $\Delta M = 2M_{up}$, where M_{up} is the branch of the magnetization loop at increasing field. Hence, $l/R = 1 - (\Delta M/2M_{up})^{1/3}$, which allows one to determine R. The ΔM and M_{up} values were measured in the field with $H_p \sim 5000$ Oe, corresponding to the field of the complete penetration of the magnetic flow in granules for these measurements. As found, the average granule radius increases from $R = 1.9$ μm μm for a sample with $x_{CuO} = 0$ to $R = 2.7$ μm for a sample with $x_{CuO} = 10\%$, where x_{CuO} is the CuO nanoparticle content. A further increase in x_{CuO} leads to a decrease in R to 2.1 μm for a specimen with $x_{CuO} = 24\%$.

The $J_c(H)$ dependences plotted in Fig. 2 were determined from the magnetization loops using the Bine formula and the above obtained R values. In comparison with $x_{CuO} = 0$, there is observed a gain in J_c for samples with $x_{CuO} = 0.5$, 1, 20, and 24%.

Figure 3 displays the critical current density J_c as a function of CuO volume content

in a $YBa_2Cu_3O_7$ HTSC ceramic. This effect of nanodispersed dopants on the critical current density can be explained by various mechanisms. In accordance with the results, adding non-superconducting CuO nanoparticles with sizes up to 10 nm in the amount of 2%, homogeneously dispersed in the matrix, enhances the pinning of the magnetic flow [1–3]. The role of nano-CuO in the increase in the critical current density is similar to the role of 211 phase inclusions [11–13] and suggests that a decrease in dimensions of these particles directly causes the higher pinning. Furthermore, these nanoparticles are believed to make no pronounced contributions to the crystalline structure of a superconducting matrix, being inert to a superconducting material. Their uniform distribution in the bulk of a superconducting matrix leads to the formation of a system of dispersed defects, which may serve as the pinning centers.

Increasing the content of non-superconducting nanoparticles to 15% within the bulk of the sample reduces naturally its superconducting properties (see Fig. 3). Nanoparticles stop playing the role of the pinning centers because of their interplay between each other. In this case, one observes the formation of the anisotropic structure with defects in the form of droplet-like inclusions, whose maximum sizes range from 90 to 120 nm (see Fig. 1b). An increase in nano-CuO concentration from 15 to 24 vol % is accompanied by a gain in the critical current density J_c. As seen in Fig. 1c, besides the droplet-like defects, there are also the mustache inclusions, whose length varies from 200 to 300 nm. The mustache is predominately represented by isotropically oriented columnar structures. According to [6], their phase composition is likely CuO. The rounding of the tip is about 10 nm. The statistical analysis of defects reveals that the average droplet structure size in the maximum cross section is 95 nm, while the base diameter of columnar structures is 100 nm at a length of 250 nm. These composites are characterized by the complex interaction of two types of defects, namely, droplets and mustache. Thus, the main contribution to the pinning force is made by the mustache defects, and the "auxiliary" pinning on the droplets impedes creep.

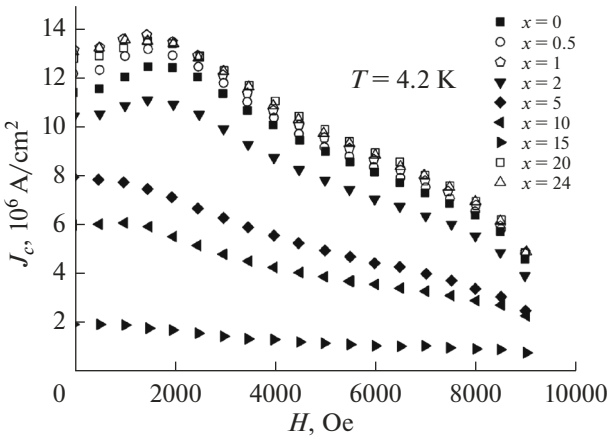

Fig. 2. Field dependence of critical current density.

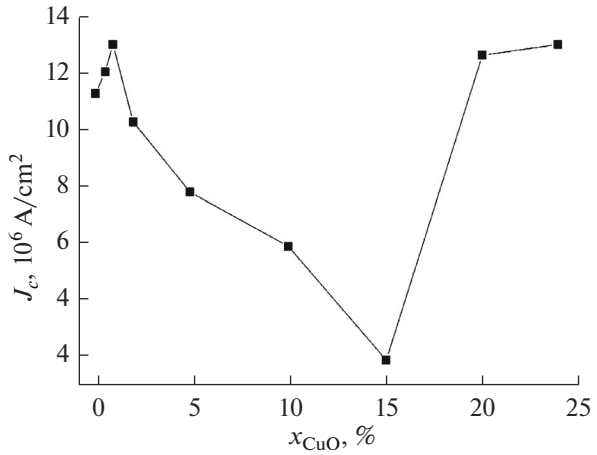

Fig. 3. J_c as a function of volume content of CuO nanoparticles.

The most efficient pinning may arise as a result of the appropriate combination of defects. The difficulty of the conception for increasing the current density is that, in spite of numerous works, there are no reliable data on the interaction between various types of defects and vortices. The aim of the present work was not the multiplication of defects, but their effective use, i.e., the combination of defects. In particular, the methods of restraining the negative effects of heat fluctuations remain almost unexplored. While the problem of obtaining defects via the introduction of

nanoparticles is currently quite solvable, the problems associated with the growth of columnar defects, such as mustache, are still poorly understood.

It is thus assumed that 2 vol % of CuO nanoparticles in a HTSC ceramic play the role of pinning centers. A further gain in the nano-CuO content within the composite causes the formation of an anisotropic structure with different defects that, depending on their structure and shape, may decrease or increase the critical current density.

The analysis of the dependence of the critical current density on the nano-CuO volume content indicates the existence of a curve allowing one to predict the optimal nanodopant concentrations. Hence, the present work clearly shows the ability to tune the critical current density J_c through the injection of nanodispersed dopants.

FUNDING

This work was supported by the Russian Science Foundation (project no. 16-19-10054).

REFERENCES

1. Kazin, P.E. and Tretyakov, Yu.D., Microcomposites based on superconducting cuprates, *Russ. Chem. Rev.*, 2003, vol. 72, no. 10, pp. 849–865.
2. Rudnev, I.A., Mikhailov, B.P., and Bobin, P.V., Magnetization and critical current of high-temperature superconductors with artificial pinning centers, *Tech. Phys. Lett.*, 2005, vol. 31, no. 2, pp. 176–178.
3. Bobylev, I.B., Gerasimov, E.G., and Zyuzeva, N.A., Influence of water vapor on the formation of pinning centers in $YBa_2Cu_3O_y$ upon low-temperature annealing, *Phys. Met. Metallogr.*, 2017, vol. 118, no. 8, pp. 738–748.
4. Kashurnikov, V.A., Maksimova, A.N., Rudnev, I.A., and Odintsov, D.S., Domain of a magnetic flux in superconductors with ferromagnetic pinning centers, *Phys. Solid State*, 2015, vol. 57, no. 9, pp. 1726–1734.
5. Troitskii, A.V., Demikhov, T.E., Antonova, L.Kh., Didyk, A.Yu., and Mikhailova, G.N., Radiation effects in high-temperature composite superconductors, *J. Surf. Invest.: X-ray, Synchrotron Neutron Tech.*, 2016, vol. 10, no. 2, pp. 381–392.
6. Ushakov, A.V., Karpov, I.V., Lepeshev, A.A., and Petrov, M.I., Enhancing of magnetic flux pinning in $YBa_2Cu_3O_{7-x}$/CuO granular composites, *J. Appl. Phys.*, 2015, vol. 118, no. 2, p. 023907.
7. Karpov, I.V., Ushakov, A.V., Lepeshev, A.A., and Fedorov, L.Yu., Plasma-chemical reactor based on a low-pressure pulsed arc discharge for synthesis of nanopowders, *Tech. Phys.*, 2017, vol. 62, no. 1, pp. 168–173.
8. Ushakov, A.V., Karpov, I.V., Lepeshev, A.A., Fedorov, L.Yu., and Shaikhadinov, A.A., Copper oxide plasmochemical synthesis for doping superconducting materials, *Materialovedenie*, 2013, no. 7, pp. 29–33.
9. Gokhfeld, D.M., Balaev, D.A., Petrov, M.I., Popkov, S.I., Shaykhutdinov, K.A., and Val'kov, V.V., Magnetization asymmetry of type-II superconductors in high magnetic fields, *J. Appl. Phys.*, 2011, vol. 109, p. 033904.
10. Landau, I.L., Willems, J.B., and Hulliger, J., Detailed magnetization study of superconducting properties of $YBa_2Cu_3O_{7-x}$ ceramic spheres, *J. Phys.: Condens. Matter*, 2008, vol. 20, no. 9, p. 095222.
11. Sengupta, S., Shi, D., Wang, Z., Biondo, A.C., Balachandran, U., and Goretta, K.C., Effect of Y_2BaCuO_x precipitates on flux pinning in melt-processed $YBa_2Cu_3O_x$, *Phys. C* (Amsterdam), 1992, vol. 199, pp. 43–49.
12. Mucha, J., Rogacki, K., Misiorek, H., Jezowski, A., Wisniewski, A., and Puzniak, R., Influence of the Y211 phase on anisotropic transport properties and vortex dynamics of the melt-textured Y123/Y211 composites, *Phys. C* (Amsterdam), 2010, vol. 470, pp. 1009–1010.
13. Su, J.H., Chintamaneni, V., Mukhopadhyay, S.M., Revur, R.R., Pyles, T., and Sengupta, S., Fabrication of thin films of multi-cation oxides ($YBa_2Cu_3O_{7-\sigma}$) starting from nanoparticles of mixed ions, *Supercond. Sci. Technol.*, 2006, vol. 19, no. 11, pp. L51–L54.

Translated by O. Maslova